JJEES

JJEES (2020) 11 (2): 103-112
ISSN 1995-6681

Jordan Journal of Earth and Environmental Sciences

Calcareous Nannofossil Biostratigraphy and Carbon Isotopes from the Stratotype Section of the Middle Eocene Wadi Shallala Formation, Northwestern Jordan

Fayez Ahmad[1*], Mahmoud Faris[2], Sherif Farouk[3]

[1]The Hashemite University, Faculty of Natural Resources and Environment, Department of Earth and Environmental Sciences, Jordan
[2]Geology Department, Faculty of Science, Tanta University, Egypt
[3]Egyptian Petroleum Research Institute, Nasr City, Egypt

Received 17 November 2019; Accepted 19 January 2020

Abstract

The stratotype section of the Wadi Shallala Formation in northwestern Jordan has been studied in this work by means of calcareous nannofossils and isotopes for the first time. In addition, the present study discusses the most important Middle Eocene calcareous nannofossil bioevents and biostratigraphy. The study section includes the upper part of Umm Rijam Chert Limestone Formation and Wadi Shallala Formation. Forty-two calcareous nannofossil species which belong to the *Nannotetrina fulgens* (NP15/CP13) Zone were recorded in the study section, and this stratotype section was assigned to the Middle Eocene age, although some previous works have assigned the lower part of this section to the Paleocene Epoch. The Umm Rijam Chert Limestone/ Wadi Shallala formational boundary is marked by the transition from the well-bedded chalk and limestone with dominated charts to the massive chalk. Chronostratigraphically, the Umm Rijam Chert Limestone / Wadi Shallala formational boundary reflects regional paleoenvironmental changes in Jordan correlatable well with nearby countries such as Egypt.

Keywords: Wadi Shallala Formation, calcareous nannofossils, isotopes, Middle Eocene, Jordan.

1. Introduction

Eocene successions in Jordan are mainly characterized by a wide shallow, open marine-rimmed carbonate platform at the southern margin of the Neo-Tethys Ocean (Powell and Moh'd, 2011). It includes the Eocene Umm Rijam Chert Limestone and Wadi Shallala formations (Figure 1).

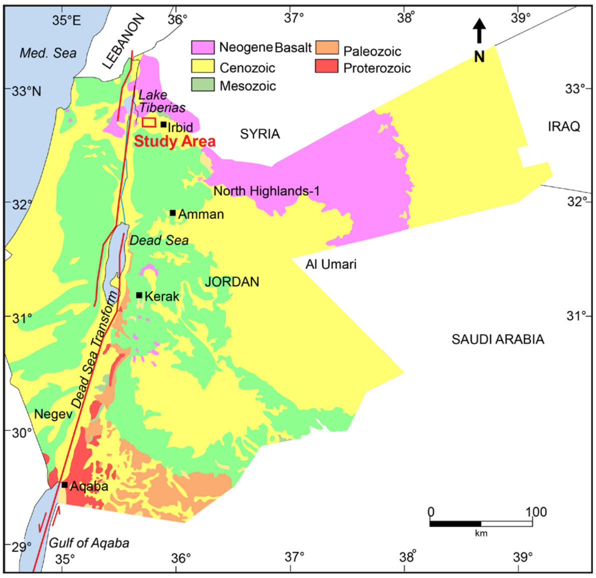

Figure 1. Regional geological map of Jordan showing the location of the study area (Al-Shawabkeh, 1991).

A long-term cooling period started at the end of the Early Eocene Cooling Event (EECO) (e.g., Bijl et al., 2010; Boscolo Galazzo et al., 2014; Hussein et al., 2015) until the Middle Eocene Climatic Optimum (~40.5 to 40 Ma; Boscolo Galazzo et al., 2014). In Jordan, the Umm Rijam Chert Limestone and Wadi Shallala formational boundary have not been previously discussed in details. Therefore, this study adds new information based on carbon isotopes and calcareous nannofossil biostratigraphy. A few previous works have focused on the Eocene microplanktonic stratigraphy of Jordan coupled with $\delta^{13}C$ and $\delta^{18}O$ isotopes (e.g., Farouk et al., 2013, 2015; Hussein et al., 2015). There is presently insufficient information for chronostratigraphy at the boundary between the Umm Rijam Chert Limestone and Wadi Shallala formations. The age assignment by the previous authors of the Umm Rijam Chert Limestone and Wadi Shallala formational boundary is a controversial stratigraphic point. It was dated to the Early-Middle Eocene (e.g., Fadda, 1996; Andrews, 1992; Sharland et al., 2004), while others reported it within the Middle Eocene (e.g., Bender, 1974; Powell and Moh'd, 2011; Farouk et al., 2013).

The main aims of the present study are: 1) to document the main Middle Eocene calcareous nannoplankton biostratigraphy and bioevents events against the $\delta^{13}C$ and $\delta^{18}O$ isotope; 2) to discuss the stratigraphic ranges of some important nannofossil species within the studied interval; and 3) to compare the obtained results with the different sections measured in west central Sinai, Egypt.

* Corresponding author e-mail: fayeza@hu.edu.jo

2. Lithostratigraphy

The exposed studied section at the type-locality of Wadi Shallala area (32°37′49″N, 35°56′23″E) includes the uppermost part of the Umm Rijam Chert Limestone and Wadi Shallala formations (Figure 2A). The Umm Rijam Chert Limestone Formation can be subdivided into three major units (Parker, 1970). The lower unit consists of about 8 m massive bituminous imparts brown-black argillaceous chalk with an unexposed base (Figure 2A). In the present study, this unit is considered to be equivalent to the Paleocene Muwaqqar Chalk Formation which was recorded in the same area by Weisemann and Abdullatif (1963) and Moh'd (2000). The middle unit consists of about 18 m thick limestone with few chert beds and nodules.The third upper unit characterizes the upper most part of the Umm Rijam Chert Limestone Formation (Figures 2B and 3). It consists of 15m thick limestone with chert intercalation. The Wadi Shallala Formation consists of about 8 m grey to white massive chalky limestone with a few chert beds/nodules towards the higher part of the studied section with observed calcium carbonate content (Figure 3). The Umm Rijam Chert Limestone/ Wadi Shallala formational boundary can be drawn above the last chert horizon, and is marked by the transition from the well-bedded chalk and limestone with dominated cherts to the massive chalk. Similar vertical facies changes were noted in Egypt between the limestone with chert of the Thebes Formation and argillaceous marl and limestone of the Darat Formation (Figure 4). The Wadi Shallala Formation is overlain by lower Oligocene limestone of the Tayba Formation in northwest Jordan and Wadi El Ghadaf in the eastern part of Jordan (e.g., Farouk et al., 2013).

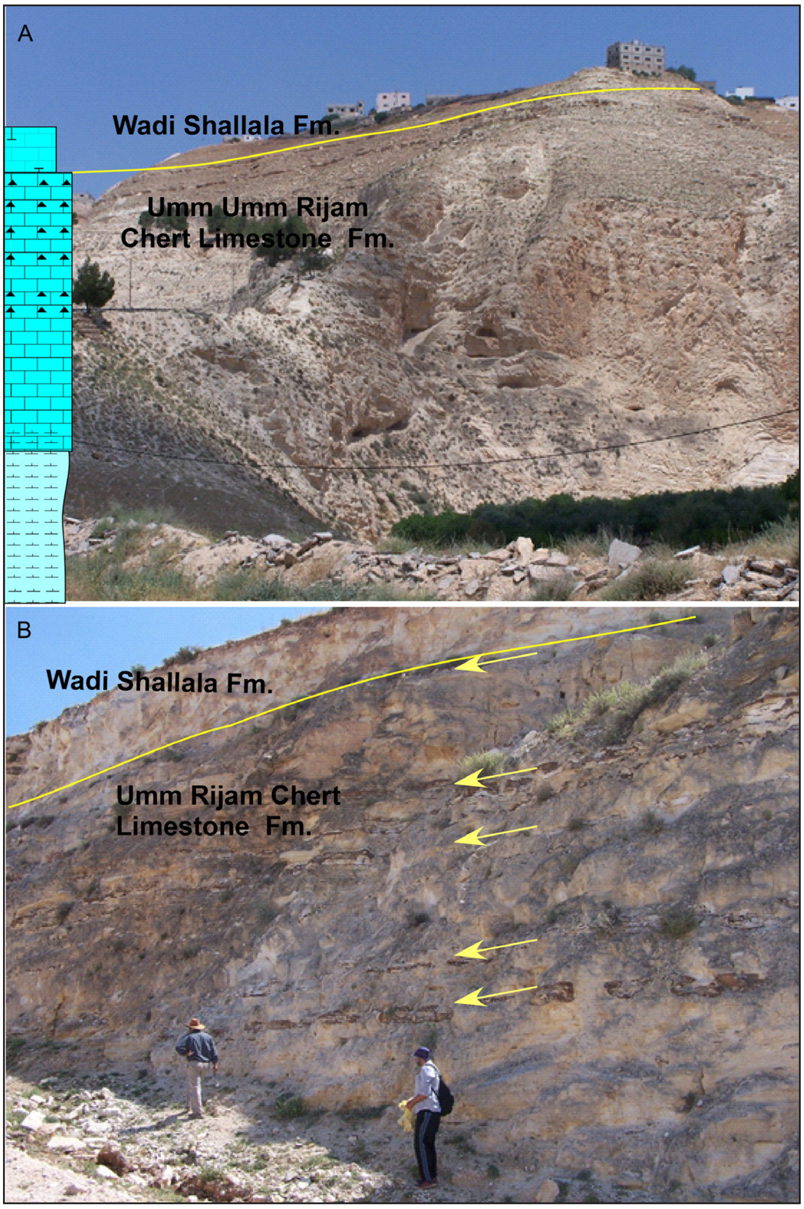

Figure 2. ***A:*** Field photograph showing the three major cycles of Umm Rijam Formation underlying the Wadi Shallala Formation. Fig. ***B:*** Field photograph showing the upper part of Umm Rijam Formation, which is characterized by an increase of bedded chert (arrows show the chert beds) underlying the massive chalk of the Wadi Shallala Formation.

3. Material and Methods

A total of 120 samples were collected, sampled, and examined for nannofossils and $\delta^{13}C$ and $\delta^{18}O$ isotope. Stable isotope analyses of $\delta^{13}C$ and $\delta^{18}O$ were performed on 120 bulk samples at the University of Arizona, Geosciences Department, Environmental Isotope Laboratory using an automated carbonate preparation device (KIEL-III) coupled with a gas-ratio mass spectrometer (Finnigan MAT 252).

Nannofossils slides were examined using the polarizing microscope with a magnification of 1250 x. Abbreviation codes used for the relative abundance of each nannofossil species are A; Abundant (1-10 Specimen/field of view) C; Common (1 Specimen / 1-10 field of view), F: Few (1 Specimen / 11-50 field of view), R: Rare (1 Specimen / 50 -100 field of view); and VR: Very Rare (1 specimen/more than 100 field of view). For preservation, an abbreviation code was used: G = good; individual specimens exhibit little or no dissolution, or overgrowth; diagnostic characteristics of most specimens are preserved and specimens are identifiable at the species level. M = moderate; individual specimens exhibit some evidence of dissolution, or overgrowth; primary diagnostic features are somewhat altered, but most specimens are identifiable at the species level. Biostratigraphic abbreviations used in the present study are: FO=First Occurrence, LO=Last occurrence.

4. Calcareous Nannofossils Biostratigraphy and Bioevents

The calcareous nannofossils in most of the studied samples are abundant to few and are well-diversified; their preservation range from good to moderate. A total of about forty-two taxa has been identified; their relative abundance, and preservation have been plotted (Table 1). Some representative nannofossil species are illustrated in Plates (1 - 2).

The biostratigraphic data obtained from calcareous nannofossils indicate that the whole studied succession is related to the *Nannotetrina fulgens* (NP15/CP13) Zone based on the zonal scheme of Martini (1971) and Okada and Bukry (1980). It is defined as the interval from the first occurrence (FO) of *N. fulgens* to the last occurrence (LO) of *Blackites gladius*. *Nannotetrina fulgens*, and other species of the genus *Nannotetrina* are used to define the base of the *N. fulgens* Zone (NP15) following the suggestions of Perch- Nielsen (1985). Perch-Nielsen (1985) and Abul-Nasr and Marzouk (1994) have remarked that the genus *Nannotetrina* disappears near the NP15/NP16 zonal boundary.

The LO of *B. infatus* and FO of *N. fulgens* together were used to trace base of *N. fulgens* Zone in the Agost section, Spain (Larrasoana et al., 2008). The FO of *N. fulgens* was used to define base of NP15a (Bown, 2005). The LO of *N. fulgens* and the FO of *Reticulofenestra umbilicus* were previously used to determine base of NP16 Zone (Perch-Nielsen, 1985). On the other hand, the NP15 (*N. fulgens*) Zone includes the interval from the FO to the LO of the nominated species (Shamrock et al., 2012). The CP13 (NP15) was divided previously by Okada and Bukry (1980) into three Subzones (CP13a, b, c).

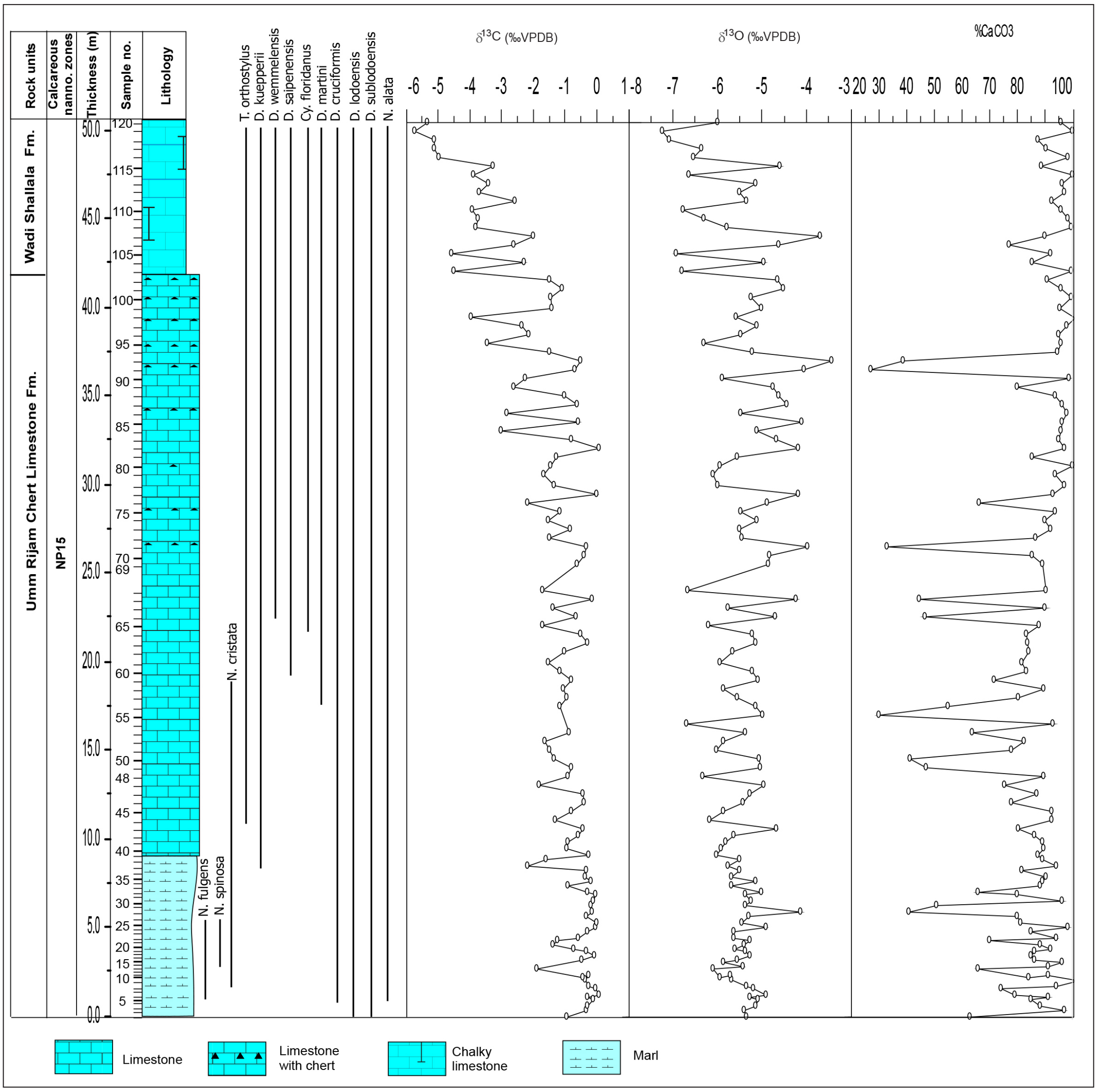

Figure 3. A measured exposed section showing the lithology against the δ13C and δ18O isotope values and CaCO3 values at the type section of Wadi Shallala Formation.

Table 1. Distribution of calcareous nannofossil species in Wadi Shallala section.

Middle Eocene																																								Age
Umm Rijam Chert Limestone Fm.																																								Formation
1	2	3	4	5	6	7	8	9	10	11	12	13	14	15	16	17	18	19	20	21	22	23	24	25	26	27	28	29	30	31	32	33	34	35	36	37	38	39	40	Sample No.
A	A	A	A	C	A	A	A	A	A	A	C	F	F	A	A	A	A	A	A	A	C	A	A	A	A	F	A	A	A	A	A	C	C	F	C	A	A	A	B	Abundance
G	M	M	M	M	M	G	G	G	G	G	G	M	M	G	M	M	G	G	M	G	G	G	G	M	M	M	M	G	G	M	M	M	M	M	G	G	G	G	-	Preservation
NP 15																																								Nannofossil zones
VR			VR	VR	VR	VR	VR	VR	VR	VR	R			VR		R	VR	R	VR	R	R	VR	VR	R	R	VR	VR	R		VR	R	R	R		R	R	VR	VR		*Campylosphaera dela*
VR		VR		VR		VR				VR	VR							VR	VR	VR		VR																		*Chiasmolithus grandis*
F	R	R	R	R	R	F	R	R	R	R	VR			R	VR	F	F	F	R	R	R	R	R	R	R	VR	F	R	F	R	F	F	R		R	F	F	R		*Chiasmolithus solitus*
VR	VR			VR	VR	VR													VR			VR			VR							VR				VR				*Discoaster sublodiensis**
R	R	R	R	R	R	R	R	R	R	F	F	VR	VR	F	F	R	R	F	R	F	F	F	F	R	R	R	F	F	F	F	F	F	F	R	R	R	R	R		*Ericsonia formosa*
VR			VR	VR		VR								VR		VR			VR	VR	VR	VR	VR	VR				VR		VR	VR	VR	VR			VR				*Neococcolithes dubius*
VR			VR			VR	VR		VR	VR					VR	VR	VR		VR	VR	VR	VR	VR	R	R	VR	R	VR	VR		VR	VR			VR	VR	VR			*Pontosphaera exilis*
VR										VR					VR					VR			VR									VR								*Pontosphaera multipora*
VR			VR			VR			VR	VR																	VR	VR	VR					VR				VR		*Pontosphaera pectinata*
VR	VR	VR				VR				VR				R	VR					VR		VR	VR				VR			VR	VR									*Pontosphaera plana*
VR	VR	VR	VR			VR	VR			R	VR			VR											VR			VR									VR			*Helicosphaera seminulum*
VR	VR		VR		VR	VR	VR	VR		VR	VR	VR	VR		VR	VR		VR	VR		VR	VR		VR			VR		VR	VR	VR	VR	VR	VR	R	R	R	R		*Sphenolithus moriformis*
R	R	R	R	VR		R	VR	VR	VR	R	R			VR	VR	R	VR	VR	VR	VR	VR	VR	R	VR	VR	VR	R			VR	VR	VR	VR		VR	VR	R	R		*Sphenolithus radians**
R	R	VR	R	F	R	R								R											VR															*Tribrachiatus orthostylus**
VR	VR	VR						VR	VR		VR			VR	VR										VR		VR								VR					*Nannotetrina alata**
VR		VR				VR					VR																													*Nannotetrina fulgens**
R	VR	VR	VR			VR	VR	VR	VR	VR		VR		VR	VR	VR		R	R	R		VR	VR	VR	VR		VR	VR	VR	VR	R	VR			R	VR	R	R		*Zygrhablithus bijugatus*
	VR			VR		R		VR			R						R	R				VR	VR	VR	VR	VR		VR	VR		VR	R	VR		R			VR		*Discoaster lodoensis**
	VR							VR			VR																													*Nannotetrina cristata**
	VR													VR		VR	VR	VR	VR	VR		VR	VR	VR	VR	VR	VR	VR	R	R	VR	VR	VR	R	R	F	F	F		*Reticulifenestra dictyoda**
		VR	VR			VR				VR																														*Scyphosphaera apsteinii*
		VR	VR				VR	VR										VR	VR	VR		VR	VR	VR	VR	VR	VR									VR				*Pontosphaera pulchra*
			VR			VR			VR		VR											VR											VR		VR		VR			*Sphenolithus editus*
				VR	VR				VR		VR			VR			VR														VR									*Discoaster cruciformis**
				VR		VR			VR		VR																													*Nannotetrina spinosa**
							VR	VR	VR								VR		VR																					*Ellipsolithus macellus*
									VR	VR							*VR*																							*Girgisia gammation*
									VR									VR		VR	VR			VR																*Discoaster barbadensis*
										VR										VR												VR								*Teweius ? crassus*
														VR	VR	VR	VR	R	R																					*Discoaster binodosus*
																R	R	R	R	F	F	F	F	R	R	R	R	R	R	R	F	F	F	VR	R	R	R	R		*Coccolithus pelagicus*
																VR										VR														*Discoaster deflandrei*
																VR	VR	VR		VR	R	VR	R	R	R		R	R	R	VR	VR	VR	R		R	R	R	R		*Helicosphaera lophota*
																	VR			VR	VR	VR		VR	VR		VR			VR		VR			VR		VR	VR		*Coronocyclus nitescens*
																	VR			VR																				*Lophodolithus mochloporus*
																		VR	VR	VR	R		VR											VR						*Discoaster kuepperi**
																		VR																						*Discoaster distichus**
																			VR	VR	VR	VR		VR	VR			VR				VR				VR				*Pontosphaera versa*
																					VR		VR																	*Sphenolithus* sp1
																							VR						VR											*Discoaster* sp1
																								VR	VR		R		R			VR		VR			R	R		*Helicosphaera sp*
																												VR									VR	VR		*Coronocyclus bramlettei*

The CP13a/NP15a includes the interval from the FO of *Nannotetrina fulgens* to the FO of *Chiasmolithus gigas*. The CP13b/NP15b (Total range subzone) represented by the interval from the FO to the LO of *Ch. gigas*. The CP13c/NP15c encompasses the interval from the LO of *Ch. gigas* to the FO of *Blackites gladius* and LO of *N. fulgens*. According to Perch-Nielsen (1985) and Bown (2005) *Discoaster sublodoensis* has its last appearance within the lower NP15 Zone. In the investigated section, *D. sublodoensis* ranges from the bottom of the section to its top (samples 1 to 120; Figure 3 and Table 1); in addition to the absence of *Ch. gigas*, this may indicate that the studied interval belongs to the lower NP15 (CP13a/NP15a).

4.1. Nannofossil Bioevents

In the present study, some nannofossil bioevents have been reported and discussed briefly as follows:

4.1.1. LO of Tribrachiatus orthostylus

The LO of *T. orthostylus* is noted as an unreliable taxon to define the top of NP13 Zone, where it has been reported within *Nannotetrina fulgens*, a marker taxon of NP15 (Perch-Nielsen, 1985; Wei and Wise, 1989). *T. orthostylus* has also been recorded within the lower NP15 Zone of the study section (from sample 1 to 26).

4.1.2. LOs of Discoaster Lodoensis and Discoaster Sublodoensis

The FO of *D. sublodoensis* defines the base of NP12; it disappears at the CP12a/NP12b (=NP14a/NP14b) (Perch-Nielsen, 1985). On the study section, *D. lodoensis* and *D. sublodoensis* ranged from sample 1 to 120, and they occurred in very rare numbers throughout the section. It is necessary to mention that both *D. lodoensis* and *D. sublodoensis* are recorded in the NP15 Zone in many sections in west central Sinai, Egypt (Strougo et al., 2003).

4.1.3. FO Nannotetrina Group

The base of NP15 is marked by the FO *Nannotetrina fulgens*, a secondary taxon used by Perch-Nielsen (1985). The total range of *Nannotetrina fulgens* is sometimes applied to delineate the lower and upper limits of the Zone NP 15

(Perch-Nielsen, 1985).

The FO of *Blackites gladius* is considered as a problematic bioevent in the eastern North Sea Basin, and consequently the upper boundary of Zone NP15 has been placed at the LO of *Nannotetrina fulgens* (Thomsen et al., 2012). The presence of *Nannotetrina fulgens* in sample (CH1) reflects the base of the Zone NP15. *Nannotetrina fulgens*, *N. spinosa, N. alata* and *N. cristata* occur in very rare frequencies throughout the study interval. The FO of *N. fulgens* and the LO of *B. inflatus* were used to trace the base of the NP15 Zone in the Agost section, Spain (Larrasoana et al., 2008)

The first appearance of *Reticulofenestra umbilicus* tentatively approximates the beginning of Zone NP16 (Perch-Nielsen, 1985), but this species does not actually appear to be present in the studied section. The authors tentatively assign the entire sampled section to Zone NP15. On the other hand, following Okada and Bukry (1980)*, Chiasmolithus gigas,* is restricted to the middle part of Zone NP 15 (NP15b/CP13b) and does not occur in the samples under study. The *N.fulgens* Zone has been reported in several sections in west central Sinai; Wadi Feiran, Hammam Faraun, and Wadi Wardan, as well as, in El Sheikh Fadl Butte (Minia-Maghagha, east of the Nile Valley) (Strougo et al., 2003).

4.1.4. LO of Discoaster kuepperii

The FO of *D. kuepperii* occurs within NP12 (Perch-Nielsen, 1985), while it's LO occurs within the upper NP14 (CP12b). In the studied section, it occurs within Zone NP15 (Sample 19 to 120). This species is previously recorded from Zone NP15 in many stratigraphic sections in west central Sinai (Strougo et al., 2003).

4.1.5. LO of Discoaster wemmelensis

Discoaster wemmelensis first appears at the base of CP12b (=NP14b), where it disappears within NP16 (Perch-Nielsen, 1985). In the present section, this species occurs within Zone NP15 (Sample 53 to 76). The LO of *D. wemmelensis* appears in the Middle Eocene sediments (NP15 Zone) in some sections in west central Sinai (Strougo et al., 2003).

Table 1. Continue

Age	Middle Eocene																																							
Rock Unit	Umm Rijam Chert Limestone Fm.																																							
Sample No.	41	42	43	44	45	46	47	48	49	50	51	52	53	54	55	56	57	58	59	60	61	62	63	64	65	66	67	68	69	70	71	72	73	74	75	76	77	78	79	80
Abundance	A	A	C	A	A	A	A	A	A	F	F	A	F	F	C	A	A	C	A	A	C	F	A	B	C	B	F	C	A	A	A	F	A	A	A	A	A	A	C	C
Preservation	G	G	M	M	G	M	M	M	M	G	G	G	G	G	G	G	G	G	M	M	G	M	M		G		M	G	G	G	G	M	M	G	G	G	M	G	M	M
Nannofossil zones	NP15																																							
Campylosphaera dela	R	VR		R	R	VR	VR	VR	VR			VR				VR	VR	VR		VR	VR	VR	VR				VR	VR	VR	VR	VR		VR	VR	VR	VR		VR		
Chiasmolithus grandis	VR			VR			VR	VR	VR										VR											VR		VR				VR		VR		
Chiasmolithus solitus	F	F	R	R	C	C	C	C	F			R	R		F	VR	R	R	F	R	R	R	F		R		R	VR	VR	F	F	R	R	F	F	F		C		R
Coccolithus pelagicus	R	R	R	VR	R	VR	R	VR	VR	VR		VR	VR	VR	VR	VR	F	F	VR	R	VR	VR	R		VR		VR	VR	VR	VR	R	VR	VR	R	R	VR	VR	VR	VR	VR
Discoaster barbadensis	VR	VR				VR	VR		VR			VR			VR	VR	VR	VR	VR	VR	VR	VR					VR		VR	VR	VR		VR	VR				VR		
*Discoaster sublodoensis**	VR	VR		VR	VR	VR	VR	VR	VR						VR	R			VR		VR	VR						VR			VR				VR					
Ericsonia formosa	F	R	R	R	R	R	R	R	R	R	R	C	F	F		R	R	R	F	R	F	R	F		F		R	F	R	R	R	R	R	F	F	R		R	R	R
Helicosphaera sp	VR	VR		VR	R			VR	VR			VR			VR										R															
Helicosphaera lophota	R	VR		VR	R	R	VR	VR											VR																					
Pontosphaera pulchra	VR			VR	VR	VR		VR				R	VR			VR	VR		VR		VR							VR	VR											
Pontosphaera versa	VR			VR	VR	VR		VR								VR	VR					VR	VR					VR		VR	VR		VR	VR		VR		VR		
*Reticulifenestra dictyoda**	F	F	F	C	F	C	F	F	F	F	R	R	R	VR		VR	R	R	F	F	VR	VR	F		R		VR	F	F	R		VR	R	R	R	R	VR	F	F	
Sphenolithus moriformis	VR		VR	VR	VR		VR	VR	VR	R	R	VR	R			VR	VR		VR		VR	VR	VR		VR		VR	VR			VR	VR				VR	VR			VR
*Sphenolithus radians**	VR	VR	R	R	VR	VR	VR	R		R	R	VR	R			R	R	R	R	R	R		R		R			R	VR	VR	VR		VR		VR	R		VR	VR	R
Pontosphaera exilis	VR	VR				VR	VR	VR	VR			R				VR		VR											VR	VR	VR	VR	VR	VR	VR	VR				
Helicosphaera bramlettei	VR	VR					VR	VR																					R											
Neococcolithes dubius	VR			VR	VR	VR	VR	VR	VR						VR	VR	VR	VR	VR	VR	VR	VR	VR					VR		VR	VR			VR		VR		VR		VR
Nannotetrina alata	VR			VR	VR					VR							VR	VR											VR											
Zygrhablithus bijugatus	VR	VR	VR	VR		VR		VR								VR				VR	VR							VR	VR	VR	VR		VR	VR		VR				VR
Discoaster binodosus		VR					VR						R					VR									VR						VR	VR	VR					
*Discoaster cruciformis**	VR	VR			VR	VR	VR	VR									VR												VR		VR									
Helicosphaera seminlum		VR			VR	VR	VR	VR	VR	VR		VR		VR	VR	VR	VR	VR	VR	VR		VR	VR		VR				VR	VR	VR		VR			VR	VR	VR	VR	VR
*Discoaster kuepperi**			VR		VR			VR							VR	VR			VR	VR	VR							VR			VR		VR	VR	VR	VR				VR
Pontosphaera multipora				VR	VR	VR	VR					VR				R											VR		VR											
Discoaster martinii				VR	VR																																			
Nannotetrina cristata				VR														VR																						
Pontosphaera pectinata				VR	VR	VR	VR	VR	VR							VR					VR								VR	VR	VR	VR	VR	VR						
Discoaster gemmifer					VR		VR		VR																		VR			VR										
Pontosphaera plana					VR			VR			VR					VR	VR													VR	VR		VR	VR	VR	VR		VR		
*Discoaster saipanensis**					VR				VR			VR				VR		VR		VR																				
Neococcolithes minutus					VR			VR																																
Sphenolithus sp1						VR									VR	VR			R																					
Discoaster deflandrei						VR			VR																													VR		
Discoaster sp						VR																					VR			VR	VR						VR			
*Discoaster lodoensis**						VR										VR		VR	VR	VR	VR	VR			VR				VR	VR	R	R	R	VR	R	R		R		
Discoaster cruciformis							VR											VR																						
Blackites tenuis							VR												VR										R	R	VR				VR			VR		
*Discoaster distichus**							VR		VR																						VR									
Discoaster wemmensis													VR						VR																	VR				
Sphenolithus sp2													VR		VR	VR			R	R																			VR	VR
Cyclicargolithus floridanus																	VR		R	R			VR		R			F	F	R	R					R	VR	F	R	R
Blackites sp																			VR											VR	R			VR		VR		VR		VR
Blackites spinous																			VR											VR	VR						VR	VR		VR
Nannotetrina spinosa																			VR	VR																				
Teweius crasus																			VR																					
Coronocyclus nitescens																				VR		VR							VR	VR				VR						
Micronstholithus attenuatus																				VR										VR				VR		VR				
Pontosphaera multipora																					R																			
*Discoaster strictus**																									VR					VR										
Girgisa gammation																									VR															
Braarudosphaera bigelowii																												VR	VR	VR	R		VR	R	VR					
Lophodolithus mochloporus																														VR										
Coronocyclus bramelttei																														VR										
Chiasmolithus grandis																															VR		VR	VR		VR				
Lophodolithus nascens																																	VR							

Table 1. Continue

Age	Middle Eocene																																							
Rock Unit	Umm Rijam Chert Limestone																					Wadi Shallala Fm.																		
Sample No.	81	82	83	84	85	86	87	88	89	90	91	92	93	94	95	96	97	98	99	100	101	102	103	104	105	106	107	108	109	110	111	112	113	114	115	116	117	118	119	120
Abundance	C	A	A	A	C	B	A	A	A	A	A	VR	C	A	A	A	A	A	A	C	A	A	R	B	F	C	C	C	C	C	C	C	VR	F	C	R	C	F	R	R
Preservation	M	G	G	G	G		G	G	M	G	G	M	M	G	G	G	G	G	G	G	G	G	M	-	G	G	G	G	G	G	G	M	M	M	G	M	M	M	M	M
Nannofossil zones	NP15																																							
Blackites sp	VR		VR	VR				VR	VR	VR	VR			VR	VR	VR			VR		VR	VR					VR													
Chiasmolithus solitus	R	F	C	F	R		R	R	F	C	F		F	F	F	F	F	F	R	C	C	C	VR		R	F	F	F	F	F		VR		VR	R	VR	F			
Coccolithus pelagicus	VR	VR	R	R	VR		VR	VR	VR	VR	R	VR	R	F	R	R	R	F	VR	VR	VR	VR	VR		VR	R	F	F	F	R	R	F	VR	F	R	R	F	F	R	R
Discoaster barbadensis	VR	VR	VR				VR	VR		VR								VR	VR		VR	VR					VR	VR		VR	VR	VR	VR	VR	VR	VR		VR		R
*Reticulifenestra dictyoda**	F	C	F	F	C		F	F	F	F	F		R	F	F	F			R	F	F	F	R		F	F	F	F	F	C	F	F		R	R		F		R	
*Discoaster kuepperi**	VR																	VR												VR										R
Ericsonia formosa	R	R	R	R	VR		R		R	R	F	VR	F	F	F	F	F	F	R	R	F	F	R		F	F	F	F	F	R	R	R		R	F	F	R	R	R	VR
Neococcolithes dubius	VR	VR	VR	VR			VR	VR	VR	VR				VR	VR		VR		VR		VR	VR				VR	VR	VR	VR	VR										
Cyclicargolithus floridanus	A	A	F	F	F		F	F	F	F	F		R	F	F	F	F	R	R	F	R	R	R		R	F	F	R	R	F	F	F		F						
Girgisa gammation	VR																																							
Coronocyclus nitescens		VR	VR	VR			VR									VR						VR					R	VR				R		VR	VR	VR	VR	VR	VR	
Chiasmolithus grandis		VR	VR	VR			VR	VR		VR	VR			VR	VR	VR	VR	VR	VR	VR	VR							VR			VR			VR	VR	VR				
Pontosphaera exilis			VR	VR				VR	VR					VR		VR			VR		VR																			
*Discoaster saipenensis**			VR																VR									VR	VR											VR
Helicosphaera lophota			VR						VR	VR			VR	VR	VR	VR			VR			VR				VR	VR													
Blackites spinosus			VR							VR	VR			VR	VR				VR		VR	VR																		
Helicosphaera seminlum			VR	R			VR	VR	VR	VR			VR	VR	VR	VR	VR	VR	VR	VR	VR	VR						VR												
*Discoaster sublodoensis**				VR					VR	VR	VR				VR	VR				VR		VR	VR						VR	VR	VR	VR			VR	R	VR			VR
Pontosphaera pectinata			VR	VR				VR	VR	VR	VR				VR		VR		VR	VR	VR	VR																		
*Sphenolithus radians**			R				VR		VR	VR					VR			VR		VR	VR				VR	VR		VR		VR		VR		VR						
Zygrhablithus bijugatus			VR	VR			VR			VR	VR				VR	VR	VR	VR	VR	VR	VR	VR			VR	VR	R			VR	VR	VR								VR
Lophodolithus mochloporus			VR																																					
Pontosphaera versa			VR							VR	VR			VR	VR	VR			VR		VR	VR																		
Pontosphaera pulchra			VR																VR			VR																		
Ellipdolithus lajollaensis			VR											VR	VR						VR	VR																		
Campylosphaera dela			VR	VR			VR				VR		VR	VR	VR							VR				VR	VR	VR												
*Discoaster lodoensis**			VR	VR			VR	VR	VR				VR		VR	VR			VR		VR						VR	VR	VR		VR				VR					VR
Ellipsolithus macellus			VR																																					
Chiasmolithus consuetus			VR																																					
Cyclicargolithus luminis					VR	VR															VR																			
Sphenolithus sp1					VR			VR																		VR														
Coronocyclus bramlettei							VR	VR	VR	VR							VR		VR	VR	VR	VR						VR												
Discoaster deflandrei								VR					VR					VR																VR						VR
*Discoaster distichus**								VR	VR																															
Discoaster gemmifer								VR																																
Discoaster binodosus								VR	VR	VR			VR									VR																		
Pontosphaera multipora									VR							VR						VR																		
Pontosphaera plana									VR				VR		VR				VR	VR		*VR*																		
Discoaster sp										VR						VR			VR															VR						VR
*Discoaster strictus**										VR									VR		VR	VR																		
Helicosphaera sp											VR					VR																								
Braarudosphaera bigelowii														VR											VR	VR					VR	VR								VR
Blackites tenuis														VR	VR	VR					VR	VR																		
Chiasmoluthus sp															VR																									
Lophodolithus nascens																VR			VR	VR																				
Sphenolithus moriformis																VR			VR	VR	VR				VR									VR			VR		VR	
Micronstholithus sp.																	VR								VR	VR														
Discoaster martini																			VR																					
*Discoaster cruciformis**																					VR							VR												VR
Neococcolithes minutus																					VR						VR	VR						VR						
Helicosphaera bramelttei																						VR																		
Nannotetrina alata																												VR												VR
*Discoaster wemmelensis**																																		VR						VR

4.1.6. FO of Discoaster saipanensis

The FO of *D. saipanensis* occurs at the base NP15 (Perch-Nielsen, 1985). It rarely occurs, and has a sporadic distribution throughout the study samples. This species has been recorded in Zone NP15 from many sections in west central Sinai (Strougo et al., 2003).

4.1.7. LO of Discoaster cruciformis

The LO of this taxon occurs around the CP12a/CP12b (NP14a/b) (Perch-Nielsen, 1985). This species has a sporadic occurrence throughout the studied samples, and its last appearance was in the topmost sample 120 (Table 1). In the west central Sinai sections, this species was previously recorded from the NP15 Zone (Strougo et al., 2003).

4.1.8. FO of Cyclogargolithus floridanus

This species is recorded from Subzone NP14b by Bown (2005). It is recognized to belong to the Middle Eocene Zone NP15 of the study section.

4.1.9. FO of Discoaster martini

The first appearance of *Discoaster martini* occurs in the lower part of Zone NP15 (Perch-Nielsen, 1985). In the present section, it first appears within Zone NP15. *D.martini* was recorded from Zone NP15 in several sections in west central Sinai (Strougo et al., 2003).

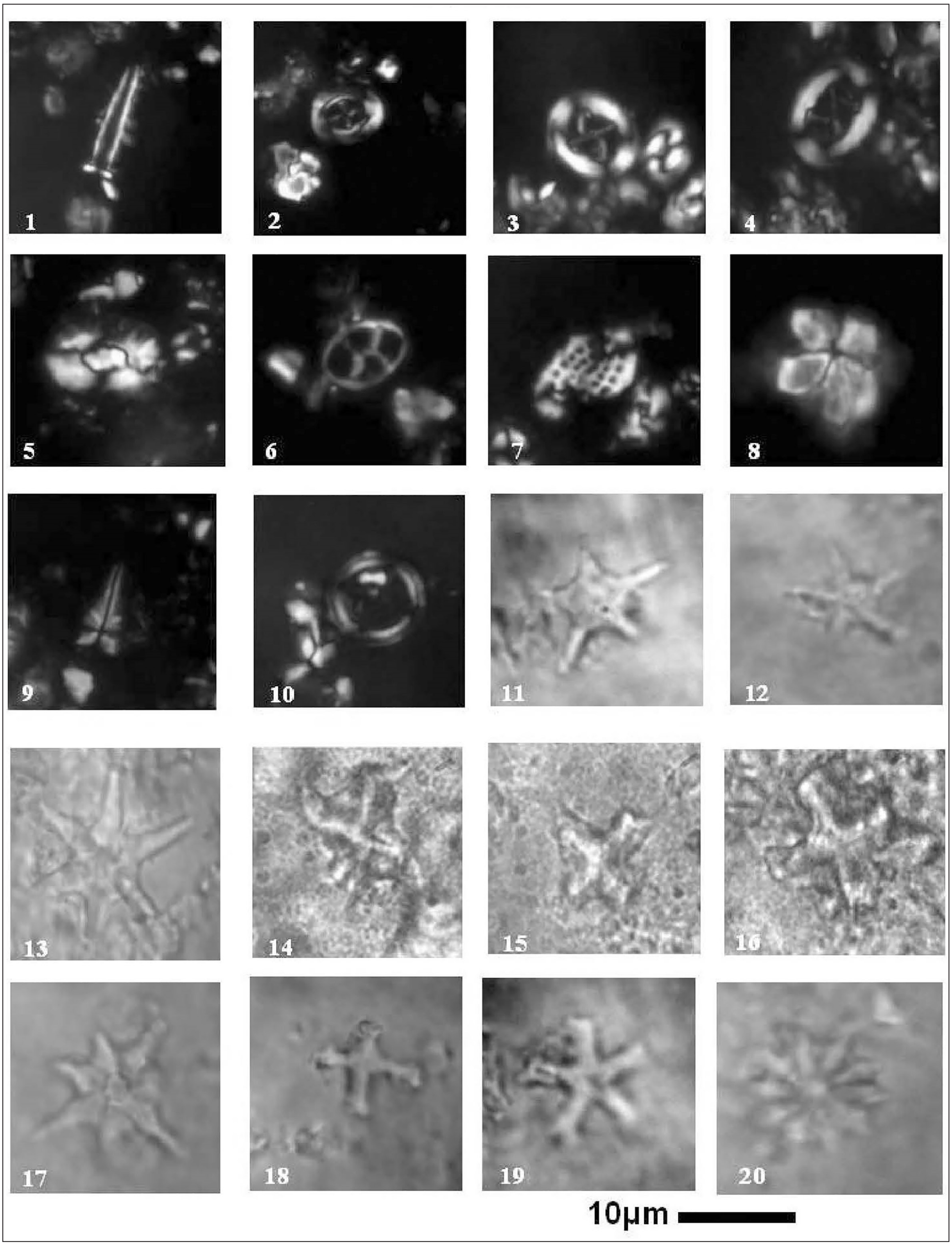

Plate 1. 1. *Blackites spinosus* (Deflandre and Fert, 1954) Hay and Towe (1962), Sample 101; 2. *Campylosphaera dela* (Bramlette Sullivan, 1961) Hay and Mohler (1967) Sample 171; 3-4. *Chiasmolithus solitus* (Bramlette and Sullivan, 1961) Locker (1968), Sample78; 5. *Helicosphaera lophota* Bramlette and Sullivan (1961), Sample 99; 6. *Neococcolithes dubius* (Deflandre, 1954) Black (1967), Sample 78; 7. *Pontosphaera multipora* (Kamptner, 1948) Roth (1970), Sample 83; 8. *Sphenolithus moriformis* (Bronnimann and Stradner, 1960) Bramlette and Wilcoxon (1967), Sample 71; 9. *Sphenolithus radians* Deflandre in Grasse (1952), Sample 59; 10. *Coronocyclus nitescens* (Kamptner, 1963) Bramletle and Wilcoxon (1967), Sample 89; 11-12. *Discoaster sublodoensis* Bramlette and Sullivan (1961); 11. Sample 1; 13. *Discoaster lodoensis* Bramlette and Riedel (1954), Sample 101; 14-15. *Nannotetrina cristata* (Martini, 1958) Perch-Nielsen (1971); 14: Sample 12; 15: Sample 2; 16. *Nannotetrina alata* (Martini, 1960) Haq and Lohmann (1976), Sample 69; 17. *Discoaster saipanensis* Bramlette and Riedel (1954), Sample 101; 18. *Discoaster cruciformis* Martini (1958), Sample 45; 19. *Discoaster martini* Stradner (1959), Sample 45; 20. *Discoaster barbadiensis* Tan (1927), Sample 102.

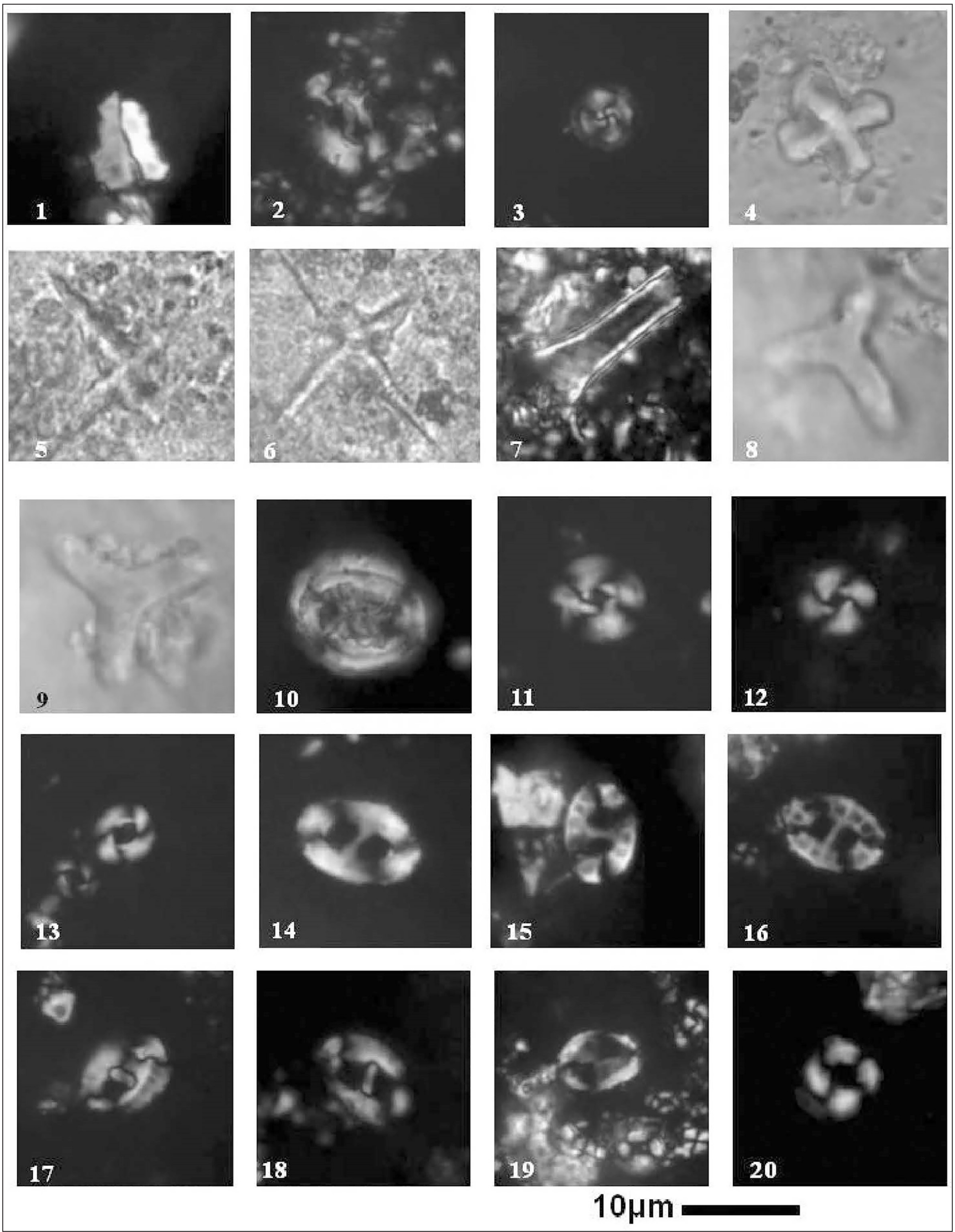

Plate 2. 1. *Zygrhablithus bijugatus* (Deflandre in Deflandre and Fert, 1954) Deflandre (1959) Sample 96; 2. *Helicosphaera bramlettei* Muller (1970), Sample 47; 3. *Girgisa gammation* (Bramlette and Sullivan, 1961) Varol (1989), Sample 10; 4. *Nannotetrina alata* (Martini, 1960) Haq and Lohmann (1976), Sample 9; 5-6. *Nannotetrina fulgens* (Stradner, 1960) Achuthan and Stradner (1969), Samples 6 and 3; 7. *Scyphosphaera apsteinii* Lohmann (1902), Sample 3; 8-9. *Tribrachiatus orthostylus* Sharmrai (1963), Samples 7 and 9; 10. *Chiasmolithus grandis* (Bramlette and Riedel, 1954) Radomski (1968) Sample 71; 11. *Cyclicargolithus floridanus* (Roth and Hay in Hay et al., 1967) Bukry (1971), Sample 83; 12-13. *Reticulofenestra dictyoda* (Deflandre in Deflandre and Fert, 1954) Stradner in Stradner and Edwards (1968); 12: Sample 42; 13: Sample 57; 14. *Pontosphaera exilis* (Bramlette and Sullivan, 1961) Romein (1979), Sample 11; 15-16. *Pontosphaera pulchra* (Deflandre in Deflandre and Fert, 1954) Romein (1979); 15: Sample 44; 16: Sample 102; 17-18. *Helicosphaera seminulum* Bramlette and Sullivan (1961); 17: Sample 61; 18: Sample 47; 19. *Pontosphaera versa* (Bramlette and Sullivan, 1961) Sherwood (1974), Sample 44; 20. *Ericsonia formosa* (Kamptner, 1963) Haq (1971), Sample 49.

5. δ^{13}C and δ^{18}O isotope

The δ^{13}C and δ^{18}O isotope record in the Wadi Shallala section shows pronounced variability on long- and short-term time scales, with δ^{13}C values ranging from -5.1‰ ‰ to 0 , while the δ^{18}O values ranged from -7 24‰ to -3.44‰ (Figure 3). The high negative values of δ^{13}C and δ^{18}O recorded in the studied section are interpreted as a late diagenetic overprint of the carbonates with no significant correlation between δ^{13}C and δ^{18}O (R^2=0.26). The δ^{13}C and δ^{18}O values decreased from -1.5 ‰ to -5.71‰ and -4.96% to -7.24% respectively, whereas the δ^{18}O records show a notable decrease near the base of the Wadi Shallala Formation. Hussein et al. (2014) reported the same negative trend for δ^{13}C and δ^{18}O isotope curves in the Jordan due to burial diagenesis as a result of observed granular calcite and drusy cements and enriched organic matter intervals.

6. Discussion and Conclusions

The calcareous nannofossil assemblage is well-diversified, and the preservation varies from good to moderate. The standard schemes of Martini (1971) and Okada and Bukry (1980) were used in this study. About forty-two nannofossil species were identified from the Middle Eocene interval of the study section including the Umm Rijam Chert Limestone and Wadi Shallala formations, which were exposed in the type-locality of Wadi Shallala, northwestern Jordan. These can be safely assigned to the *Nannotetrina fulgens* Zone (NP15) for the whole stratigraphic section. The abundance of nannotetrinids is very rare throughout the study interval with a discontinuous distribution. Okada and Bukry (1980) have divided Zone CP13 (=NP15) into three subzones (a, b and c). The lowest Subzone CP13a includes the interval from the FO of *N. fulgens* to the FO of *Chiasmolithus gigas*. The middle Subzone CP13b includes the total range of *Ch. gigas*, and the younger Subzone CP13c occupies the interval from the LO of *Ch.gigas* to the LO of *N. fulgens*. Owing to the entire absence of *Ch. gigas* (a marker of subzone CP13b) and *R. umbilicus* (marker of base NP16), and the continuous presence of *D. lodoensis*, *D. sublodoensis* throughout the samples studied (samples from 1 to 120), it can be concluded that the section under study can be assigned to the Subzone NP15a. Some of the Middle Eocene nannofossil events of Martini (1971) and Okada and Bukry (1980) have been recognized. The stratigraphic ranges of some important nannofossil markers are also briefly discussed. In the present study, the Umm Rijam Chert Limestone and the overlying Wadi Shallala formational boundary occurs the nannofossil NP15 /CP13 Zone. A vertical facies change is assignable within Zone NP15 either in Egypt and Jordan covering a wide disruption which reflects a eustatic sea-level change. So, the upper part of the Umm Rijam and the Wadi Shallala formations in the study area are well-correlated with the upper part of the Thebes Formation (similar to the lithology of Umm Rijam Chert Limestone Formation) and overlying Darat Formation (which consists of argillaceous limestone with marl) in west Sinai of Egypt (Figure 4).

At the Wadi Shallala section, the δ^{13}C and δ^{18}O isotope values show a clear negative excursion in δ^{13}C and δ^{18}O measurements near the lower part of the Shallala Formation implying a different diagenetic process.

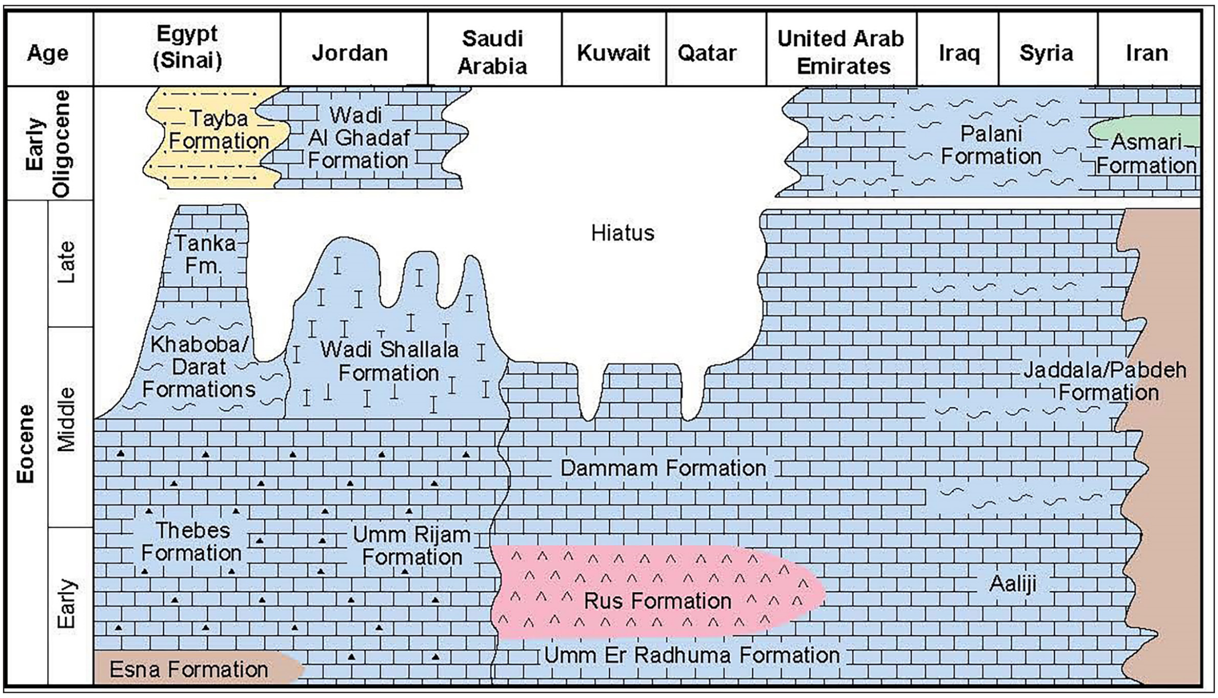

Figure 4. Comparison of Umm Rijam and Wadi Shallala formations with others lithostratigraphic schemes for the Paleogene succession across the African/Arabian plates (modified after Sharland et al., 2001; Farouk et al., 2013 and 2015).

Acknowledgements

The financial support provided by The Hashemite University to Dr. Fayez Ahmad is gratefully acknowledged. Comments by three anonymous reviewers greatly improved an earlier draft of the manuscript.

References

Abul-Nasr, R.A. and Marzouk, A.M. (1994). Eocene biostratigraphy of Wadi Wardan, Sinai, with especial Emphasis on calcareous nannofossils. M.E.R.C. Ain Shams Univ, Earth Sci. Ser. 8:178-187.

Al-Shawabkeh, K. (1991). The geology of the Adir area. Map sheet no. 3152 II. Bull. 18, Amman.

Andrews, I. J. (1992). Cretaceous and Paleogene lithostratigraphy in the subsurface of Jordan. Natural Resources Authority Subsurface Geol. Bull. 5, P. 60.

Bender, F., (1974). Geology of Jordan. Gebrueder Borntraeger, Berlin, P. 196 p.

Bijl, P. K., Houben, A. J. P., S. Schouten, S., Bohaty, S. M., Sluijs, A., Reichart, G. J. J. S. Sinninghe Damsté, J. S. S., Brinkhuis, H. (2010), Transient middle Eocene atmospheric CO2 and temperature variations. Sci. 330 (6005): 819–821.

Boscolo Galazzo, F., Thomas, E., Pagani, M., Warren, C., Luciani, V., Giusberti, L. (2014). The middle Eocene climatic optimum (MECO): A multiproxy record of paleoceanographic changes in the southeast Atlantic (ODP Site 1263, Walvis Ridge). Paleoceanogr. 29: 1143-1161.

Bown, P.R. (2005). Palaeogene calcareous nannofossils from the Kilwa and Lindi areas of coastal Tanzania (Tanzania Drilling Project 2003-4). Jour. Nannoplankton Res. 27(1): 21-95.

Fadda, I. (1996). The Geology of Wadi El Ghadaf Area Map Sheets No. 3353-II. The Hashemite Kingdom of Jordan, Natural Resources Authority, Geological Mapping Division, Bull. 34 p. 26.

Farouk, S., Ahmad, F., Smadi, A. (2013). Stratigraphy of the middle Eocene – lower Oligocene successions in northwestern and eastern Jordan.-Jour. of Asian Earth Sci. 73: 396–408.

Farouk, S., Faris, M., Ahmad, F., Powell, J. (2015). New microplanktonic stratigraphic data and sequences across the Middle-Late Eocene and Oligocene boundaries in eastern Jordan. GeoArabia 20 (3): 145-172.

Hussein, M.A., Alqudah, M., Blessenohl, M., Podlaha, O., Mutterlose, J. (2015). Depositional environment of Late Cretaceous to Eocene organic-rich marls from Jordan. GeoArabia 20 (1):191-210.

Hussein, M.A, Alqudah, M., Boorn, S., Kolonic, S., Podlaha, O., Mutterlose, J. (2014). Eocene oil shales from Jordan -their petrography, carbon and oxygen stable isotopes. GeoArabia 19 (3): 139-162.

Larrasoana, J.C., Gonzalvo, C., Molina, E., Monechi, S., Ortiz, S., Tori, F., Tosquella, J. (2008). Integrated magnetobiochronology of the Early/Middle Eocene transition at Agost (Spain): Implications for defining the Ypresian/ Lutetian boundary stratotype. Lethaia 41 (4): 395-415.

Martini, E., (1971). Standard Tertiary and Quaternary calcareous nannoplankton zonation. In: Farinacci, A. (Ed.): proceeding II Plan Conf, Roma, 1970, 2: 739-785.

Moh'd, B. (2000). The geology of Irbid and Ash Shuna Ash Shamaliyya (Waqqas) map sheet no. 3154-II and 3154-III. Natural Resources Authority, Geol. Mapping Division, Bull. 46.

Okada, H. and Bukry, D. (1980). Supplementary modification and introduction of code numbers to the low latitude coccolith biostratigraphic zonation (Bukry, 1973; 1975). Marine Micropaleontol. 5: 321-325.

Parker, D.H., (1970). The hydrogeology of the Mesozoic-Cenozoic aquifers of the western highlands and plateau of east Jordan. UNDP/FAO, AG 2: SF (No. 2). Jordan 9, Technical report.

Perch-Nielsen, K. (1985) Cenozoic Calcareous Nannofossils. In: Bolli, H.M., Sanders, J.B. and Perch-Nielsen, K. (Eds.), Plankton Stratigraphy, Cambridge University Press, Cambridge, 427-554.

Powell, J.H. and Moh'd, B.K. (2011). Evolution of Cretaceous to Eocene alluvial and carbonate platform sequences in central and south Jordan. GeoArabia 16 (4): 29-82.

Shamrock, J.L., Watkins, D.K., Johnston, K.W. (2012). Eocene biogeochronologyand magnetostratigraphic revision of ODP Hole 762C, Exmouth Plateau (Northwest Australian Shelf). Stratigraphy 9 (1): 55–75.

Sharland, P.R., Archer, R., Casey, D.M., Davies, R.B., Hall, S.H., Heward, A.P., Horbury, A.D., Simmons, M.D. (2001). Arabian Plate Sequence Stratigraphy. GeoArabia Special Publication 2, P. 371.

Sharland, P.R., Casey, D.M., Davies, R.B., Simmons, M.D., Sutcliffe, O.E., (2004). Arabian plate sequence stratigraphy revisions to SP2. GeoArabia 9 (1): 199–214.

Strougo, A., Faris, M., Basta, R.K. (2003). Dating the "Cardita Limestones" and the lower "Green Beds" of west central Sinai by calcareous nannofossils. M.E.R. C. Ain Shams Univ. Earth Sci. Ser. 17:87-114.

Thomsen E, Abrahamsen N, Heilmann-Clausen C, King C, Nielsen O. B. (2012). Middle Eocene to earliest Oligocene development in the eastern North Sea Basin: Biostratigraphy, magnetostratigraphy and palaeoenvironment of the Kysing-4 borehole, Denmark. Palaeogeogr. Palaeoclimatol. Palaeoecol. 350–352:212–235. doi: 10.1016/j. palaeo.2012.06.034.

Wei, W., and Wise S.W. Jr. (1989). Paleogene calcareous nannofossil magnetobiochronology: results from South Atlantic DSDP site 616. Mar. Micropaleontal. 14:119–152.

Weisemann, G., and Abdullatif, A. (1963). Geology of the Yarmouk area, North Jordan. GGM report, P. 81.